Supplementary Information (SI) for Journal of Materials Chemistry C.
This journal is © The Royal Society of Chemistry 2025

1 # Preparation of High Gain NIR Photodetectors Based on Gradient $AgInS_2$(Se) Thin
2 Films with A W^{-1} Level Responsivity

3 Genglong Chen[1,2], Jiang Cheng[1*], Chenenze Jiang[3], Qingquan Ye[1], Xiang meng[1], Hua Tang[1], Fuqiang Zhai[1], Lu Li[1*]
4
5 G. Chen, J. Cheng, Q. Ye. X. Meng, H. Tang, F. Zhai, L Li
6 [1]School of Materials Science and Engineering, Chongqing University of Arts and Sciences, Chongqing 402160, P. R. China
7 Email: lli@cqwu.edu.cn (L. Li)
8 G. Chen
9 [2]School of materials science and Engineering, Chongqing University of Technology
10 Chongqing 402160, P. R. China
11 Email: c714525828@hotmail.com (G. Chen)
12 C. Jiang
13 [3]Department of Physics & Astronomy, University College London, Senate House, Malet Street, London WC1E 7HU.
14 Email: zcapcj0@ucl.ac.uk (C. Jiang)

15 **Keywords**: Near-infrared detector; Spray pyrolysis deposition; Vertical heterojunction; Silver indium sulfide; Selenization
16
17

18 ## 1 Experiment

19 ### 1.1 Materials

20 Silver nitrate ($AgNO_3$, ≥99.95%) was purchased from Knowles. Cadmium sulfate ($CdSO_4$, 99.99%), and thiourea (CH_4N_2S,
21 99%), Indium nitrate hydrate ($In(NO_3)_3\cdot 2H_2O$, 99.9%) was sourced from Macklin. Ethylene glycol monomethyl ether ($C_3H_8O_2$,
22 >99.5%), ammonia water (NH_4OH), and selenium powder (Se, ≥99.99%) were procured from Aladdin. Thiourea (CH_4N_2S, 99%)
23 for the $AgInS_2$ solution was obtained from Thermo Scientific.
24

25 ### 1.2 Preparation of gradient $AgInS_2$(Se) films

26 Initially, an $AgInS_2$ precursor film is synthesized atop the CdS layer by employing ultrasonic spray pyrolysis (USP) with a
27 deposition rate of 180 nm/min. The spray solution is concocted as follows: 0.8 mmol of silver nitrate, 0.8 mmol of indium nitrate,
28 and 1.6 mmol of thiourea are dissolved in 7.5 ml of ethylene glycol monomethyl ether. Thereafter, 0.08 ml of nitric acid is introduced
29 into the mix to enhance dissolution and prevent hydrolysis. During the USP procedure, the nozzle is positioned 30 mm above the
30 glass on the heated template. Nitrogen gas with a flow rate of 20 L/min is employed as the carrier, and the atomization rate of the
31 solution is set to 0.35 mL/min. After the spraying process, the fabricated $AgInS_2$ precursor film undergoes a thermal selenization

process within a controlled, dual-temperature rapid thermal processing (RTP) furnace, where selenium powder is heated to 350°C, and the precursor film to 380°C for varied time intervals.

1.1 Device Fabrication

The glass substrate (4×5 cm^2) coated with indium tin oxide (ITO) is cleaned using ultrasonic methods. The $AgInS_2$(Se) device is assembled in a sequential order based on the structure: ITO/CdS/$AgInS_2$(Se)/Au. A 100 nm thick CdS buffer layer, with its thickness slightly surpassing that of the depletion region, is precisely deposited onto the ITO substrate through the chemical bath deposition (CBD) technique at 80°C for 7 minutes, followed by annealing at 400°C for 10 minutes. The CBD solution is prepared as follows. Two separate solutions are created by dissolving 1.717 mg of thiourea and 1.071 mg of cadmium sulfate in 30 ml of ultrapure water, respectively. These solutions are subsequently mixed with 210 ml of deionized water, 30 ml of ammonia water to form the reaction solution. An $AgInS_2$(Se) film is then prepared on the CdS layer. Finally, an 80 nm-thick patterned Au electrode is sputtered onto the $AgInS_2$(Se) film's surface through a shadow mask.

1.2 Materials Characterization and Device Test

The surface and interface morphology, together with the elemental distribution of the material, were investigated using high-resolution field-emission scanning electron microscopy (SEM, Zeiss Merlin) equipped with energy-dispersive X-ray spectroscopy (EDX, Oxford Instruments). The phase composition of the film was analyzed using a multifunctional high-resolution X-ray diffractometer (XRD, PANalytical/Empyrean). Absorption spectra were obtained with a UV–Vis–IR spectrophotometer (Agilent Cary 5000). The electronic structure was probed using X-ray photoelectron spectroscopy (XPS, Thermo ESCALAB 250Xi). Film thickness measurements were performed using a stylus profilometer (Alpha-Step D-100). Device performance was evaluated by recording the J-V characteristics under various illumination conditions with a Keithley 2450 source meter. The photocurrent response upon light exposure was measured with a Keithley 2450 source meter; the light's on/off cycle and interval were managed by a relay-operated controller. Pulse testing was executed under 660 nm illumination. Additionally, transient photovoltage and frequency response to 660 nm laser excitation were captured using an oscilloscope.

(a) Distribution Chart Total Spectrum

element	Atomic percentage
S	38.62
Se	7.07
Ag	28.32
In	25.98
total:	100.00

(b) Distribution Chart Total Spectrum

element	Atomic percentage
S	32.05
Se	14.34
Ag	27.59
In	26.02
total:	100.00

(c) Distribution Chart Total Spectrum

element	Atomic percentage
S	16.57
Se	30.33
Ag	27.04
In	26.06
total:	100.00

(d) Distribution Chart Total Spectrum

element	Atomic percentage
S	13.87
Se	33.17
Ag	27.18
In	25.78
total:	100.00

(e) Distribution Chart Total Spectrum

element	Atomic percentage
S	6.45
Se	26.01
Ag	32.66
In	34.88
total:	100.00

(f) Distribution Chart Total Spectrum

element	Atomic percentage
S	6.56
Se	40.95
Ag	26.65
In	25.84
total:	100.00

(g) Distribution Chart Total Spectrum

element	Atomic percentage
S	6.38
Se	41.67
Ag	26.70
In	25.25
total:	100.00

(h) Distribution Chart Total Spectrum

element	Atomic percentage
S	5.18
Se	41.01
Ag	27.50
In	26.31
total:	100.00

(i) Distribution Chart Total Spectrum

element	Atomic percentage
S	4.50
Se	44.41
Ag	26.27
In	24.81
total:	100.00

Figure S1. EDS analysis of $AgInS_2$(Se) thin films with varying selenization time. Selenization conducted for (a) 5 min, (b) 8 min, (c) 10 min, (d) 15 min, (e) 20 min, (d) 25 min, (d) 30 min, (d) 35 min and (f) 40 min.

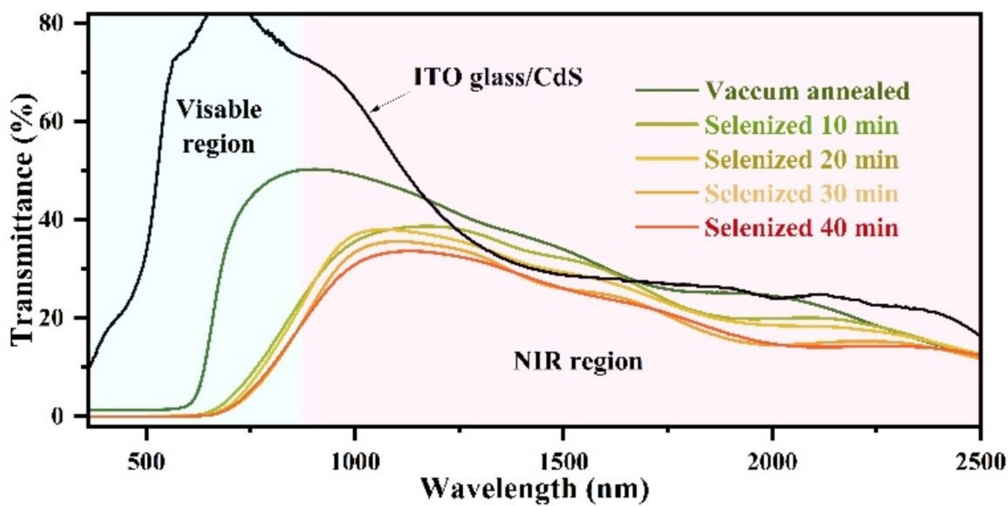

Figure S2. Transmittance spectra of $AgInS_2$ (Se) thin films with different selenization times.

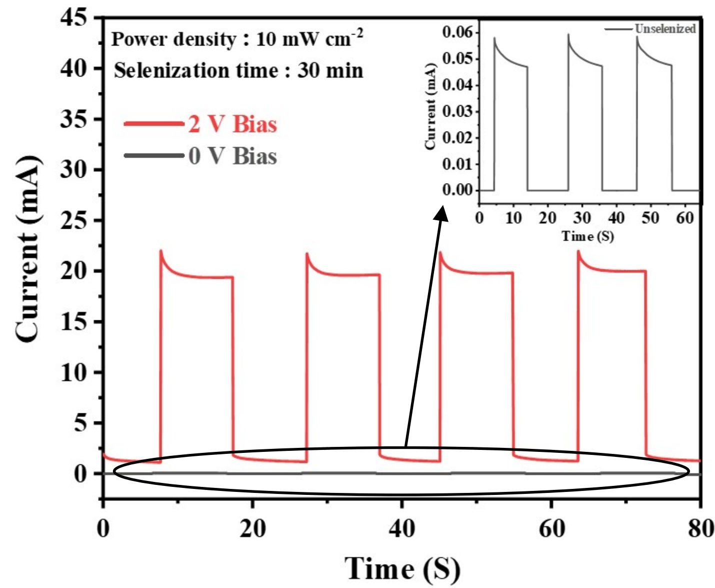

1
2 **Figure S3.** Photo-response of annealed and selenized devices to 660 nm light at 0 V and 2 V reverse bias.
3
4
5 **Table S1.**
6 The photodetection parameters of annealed and selenized devices

Illumination（nm）	Treatment	660	760	800	850	900	940	980	1050
Responsivity ($A W^{-1}$)	Vacuum annealed	1.00E-02	2.00E-03	4.30E-04	2.40E-05	1.64E-05	6.72E-06	4.45E-06	2.85E-06
	Selenzied	1.25E-01	2.50E-02	2.00E-02	1.75E-02	1.45E-02	1.33E-02	9.25E-03	8.00E-03
EQE	Vacuum annealed	1.88E-02	3.27E-03	6.60E-04	3.51E-05	2.27E-05	8.89E-06	5.64E-06	3.37E-06
	selenzied	2.35E-01	4.09E-02	3.11E-02	2.56E-02	2.00E-02	1.75E-02	1.17E-02	9.47E-03
Detectivity (jones)×10^9	Vacuum annealed	2.770	0.554	0.118	0.012	0.008	0.003	0.002	0.001
	Selenzied	8.650	2.290	1.490	1.160	1.080	0.990	0.691	0.553

7

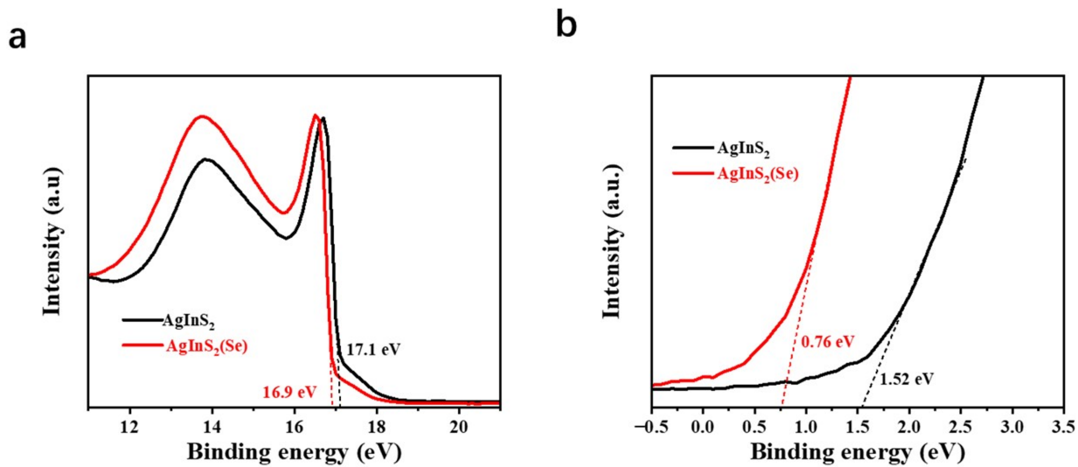

8
9 **Figure S4.** The UPS spectra of $AgInS_2$ and $AgInSe_2$ were analysed to determine (a) the valence band onset (VBO) and (b) the cut-

1 off region.

2

3 **Table S2.** The relevant level parameters of $AgInS_2$ (Se) /CdS heterojunction

Sample	E_g (eV)	VBO (eV)	W_F (eV)	Ec (eV)	Ev (eV)
CdS	2.4	2.3	4.38	-4.28	-6.68
$AgInS_2$	1.84	0.93	4.10	-3.19	-5.03
$AgInSe_2$	1.07	0.84	4.30	-4.07	-5.14

4

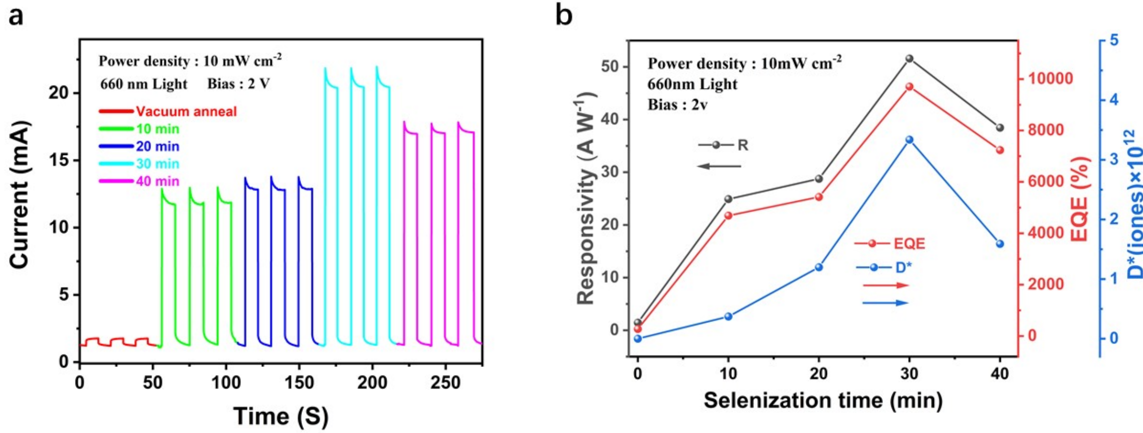

5

6 **Figure S5.** Variation of photodetector parameters with different selenization time under 660 nm light irradiation. (a) I-t
7 characteristics, and (b) photodetection parameters.

8

9

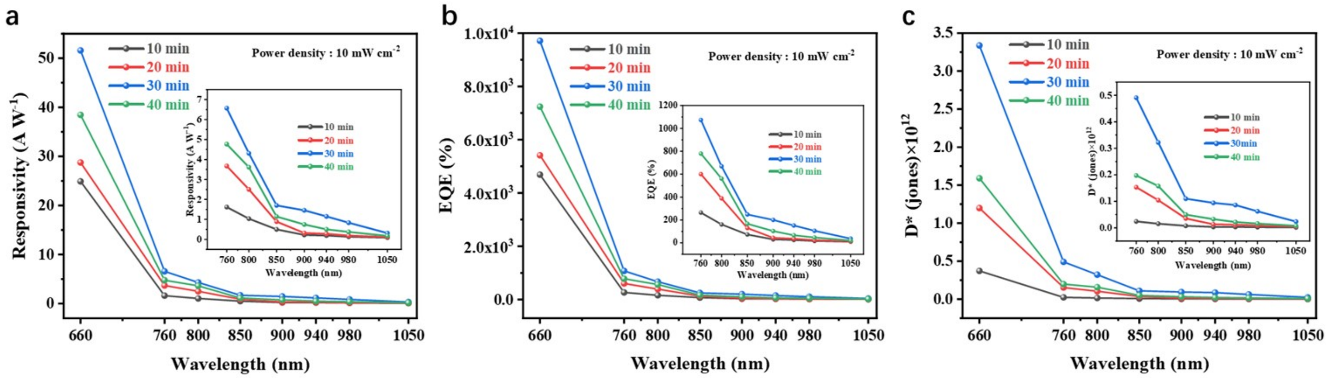

10

11 **Figure S6.** Variation of important photodetection parameters of devices with different selenization time tested under various
12 wavelengths of light. (a) R, (b) EQE and (c) D*.

13

14

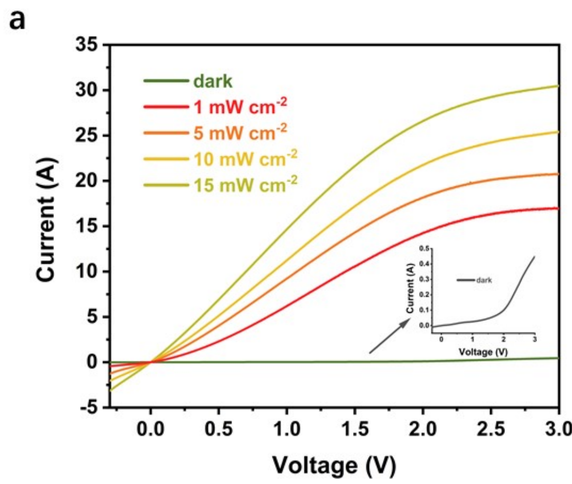

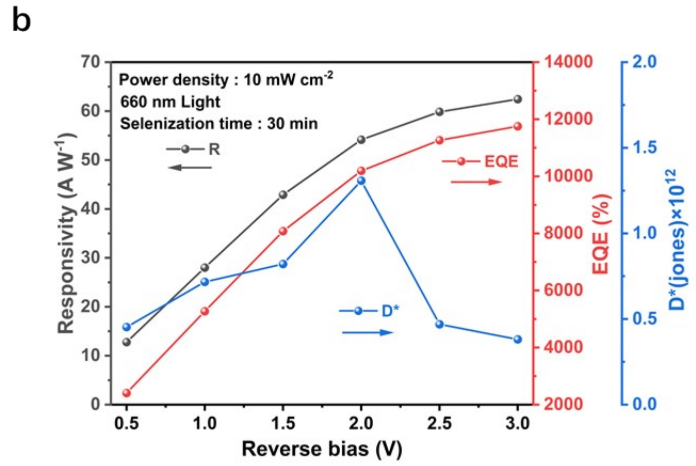

Figure S7. Performance of the $AgInS_2$(Se) thin-film photodetector irradiated with 660 nm light at different reverse bias. (a) I-V characteristic, (b) photodetector parameters.

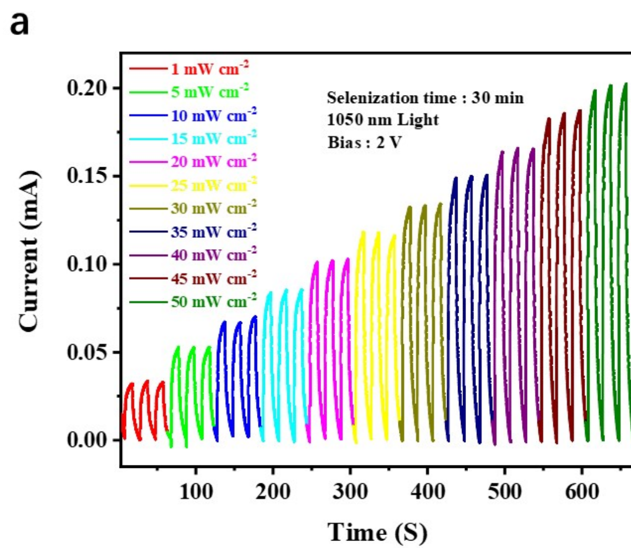

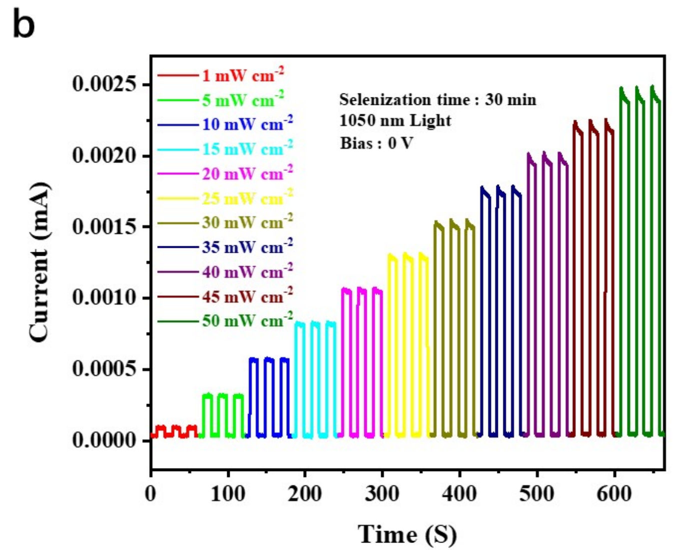

Figure S8. I-t characteristics of devices illuminated with 1050 nm light at various power densities. (a) at 2 V reverse bias and (b) at 0 V.

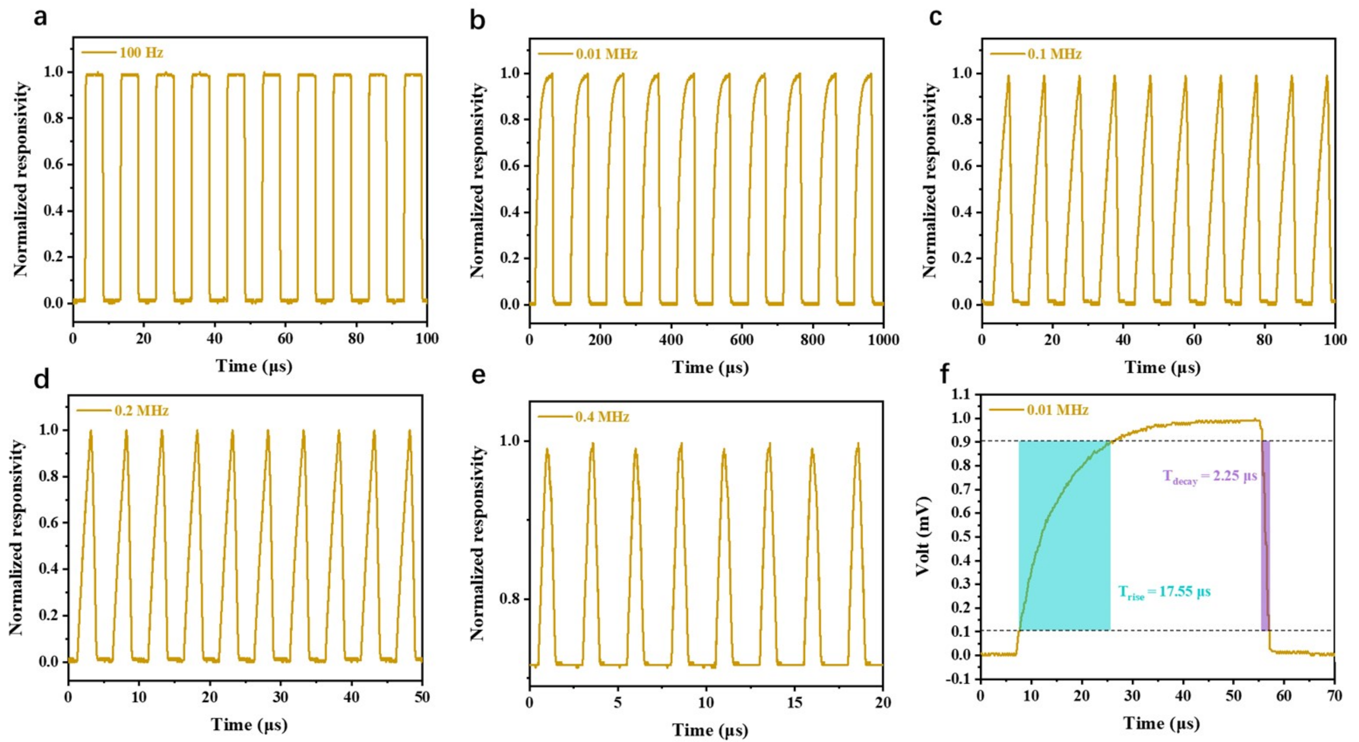

Figure S9. Frequency response of a commercial Ge detector (GPD GM6VHS) to a 660 nm laser. the response of a ge detector to a square wave incident light source at frequencies of (a) 100 Hz, (b) 10 kHz, (c) 100 kHz, (d) 200 kHz, (e) 400 kHz, and (f) the response time of the photodetector.

Table S3.
Photocurrent measurement of the device underneath ripe and unripe kiwifruit irradiated with light at different wavelengths.

Wavelength / **Maturity**	660 nm	760 nm	800 nm	850 nm	900 nm	940 nm	980 nm	1050 nm
Current (**Ripe**) (μA)	27.4	7.3	4.0	1.8	0.8	0.4	0.1	0.1
Current (**Unripe**) (μA)	5.5	2.3	1.4	0.7	0.3	0.1	-	-

Table S4.
Photocurrent response of the device under ten groups of ripe and unripe kiwifruit irradiated with 660 nm light.

Samples / **Maturity**	1	2	3	4	5	6	7	8	9	10
Current (**Ripe**) (μA)	18.0	23.1	26.7	25.0	24.2	20.0	23.1	18.8	24.1	22.0
Current (**Unripe**) (μA)	13.0	12.5	14.0	11.6	12.6	13.2	10.0	15.0	12.4	12.0

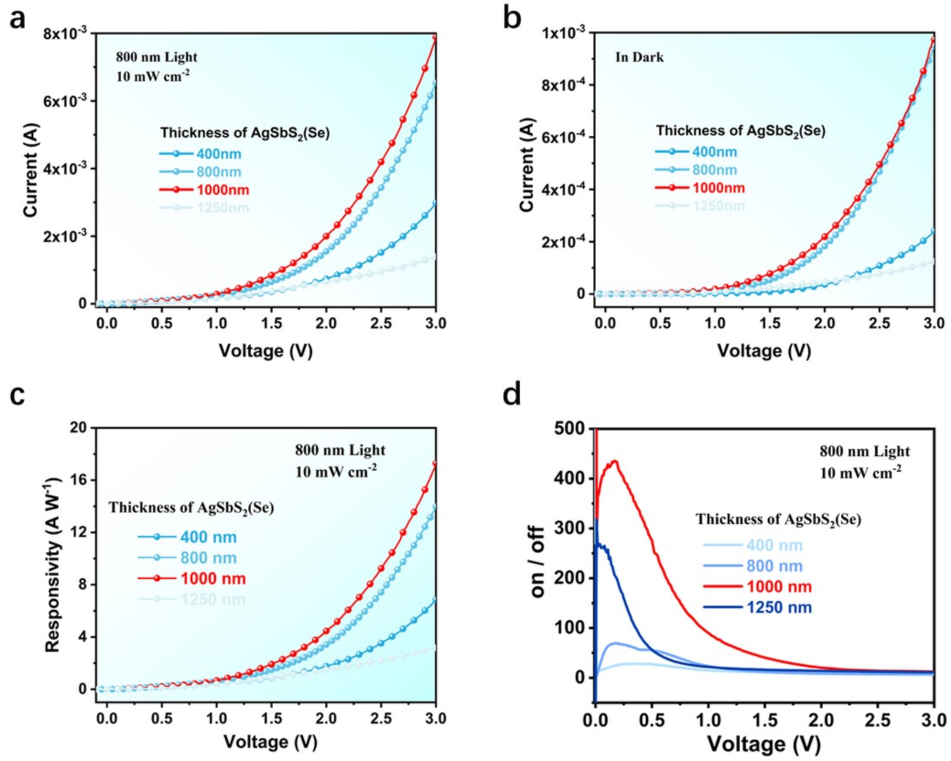

1
2 **Figure S10.** Device performance varies with $AgInS_2$(Se) thickness. (a) I-V characteristics (a) under 800 nm illumination and (b) in
3 the dark for devices with $AgInS_2$(Se) film thicknesses of 400 nm, 800 nm, 1000 nm, and 1250 nm. (c) Responsivity and (d) on/off
4 ratio of devices with varying $AgInS_2$(Se) thicknesses under different reverse bias conditions.
5